Tellus (1995), 47A, 941–954
Printed in Belgium – all rights reserved

Copyright © Munksgaard, 1995
TELLUS
ISSN 0280–6495

Interannual and decadal variations of blocking activity in a quasi-geostrophic model

By QING LIU* and THEO OPSTEEGH, *Royal Netherlands Meteorological Institute, P.O. Box 201, 3730AE De Bilt, The Netherlands*

(Manuscript received 5 April 1994; in final form 4 January 1995)

ABSTRACT

Blocking regimes simulated in a spectral 3-level quasi-geostrophic model have been examined and compared with observations. A control experiment and perturbation experiments have been performed using different constant and time-varying external forcing fields. The main emphasis of this paper is to determine the signal to noise ratio of the effects of anomalous external forcing and the natural variations in blocking activity. Forcing the model with the climatological winter mean external forcing, a control experiment has been carried out for 500 winters. The model simulates accurately the structure of the blocking pattern, as well as its effect on the transient weather systems. It also produces approximately the same number of blocking days as in the observations. However, the average duration of the simulated blocking regimes is about one day shorter than the observed one. The interannual variability in blocking activity is similar to the observations. The model also produces substantial long-term variations in blocking activity on a time-scale of decades. The observed climatological intraseasonal variations in the external forcing field appear to have a negligible effect on the mean blocking activity and its interannual variability. Observed interannual changes in the forcing configuration significantly affect the probability for a blocking circulation to occur. However, if we include the year-to-year changes in external forcing, the model generates only slightly larger interannual variations in blocking activity as compared to the control experiment with constant climatological forcing. So it seems that the observed interannual variability of blocking in winter is predominantly internally generated and changes in external forcing fields are of secondary importance.

1. Introduction

A significant part of atmospheric low-frequency variability is that associated with the interannual variations in the occurrence of blocking. The character of individual months or even seasons can be predominantly determined by the occurrence or non-occurrence of blocking in middle and high latitudes. The observed interannual variations in the occurrence of blocking may be considered to consist of two parts. One part simply reflects the complex dynamical properties of the atmosphere. Low-frequency variability can arise naturally as a result of the nonlinear internal dynamics of the atmosphere. The other part results from changes in the boundary conditions, which is referred to as the external forcing in this paper. Although earlier studies have indicated that both the external forcing and the internal dynamics of the atmosphere may play a role in causing interannual variations in the occurrence of blocking, a clear picture is still lacking. Namias (1964) suggested that anomalies in the North Atlantic sea surface temperatures (SST) and the cold-season snow cover over Scandinavia are important ingredients for the frequent and persistent blocking activity over Northern Europe during all seasons from late 1958 through early 1960. White and Clark (1975) have related the blocking activity over the North Pacific to the sensible heat flux from the underlying water. They found them to be negatively correlated. In a general circulation model (GCM) experiment, Mullen (1989) investigated the impact of Pacific

* Corresponding author.

SST anomalies on blocking activity over the North Pacific ocean. He found that Pacific SST anomalies do not strongly affect the total number of blocking days in the North Pacific basin, but they do affect the preferred regions where blocking ridges are likely to occur in the basin. Although these studies indicate that anomalies in external forcing do play a role in generating interannual variations in blocking activity, the signal to noise ratio of the effects of external forcing as compared to the natural low-frequency variability of blocking is not investigated. Many studies (Lau, 1981; Manabe and Hahn, 1981; Chervin, 1986) have shown that even without any anomalous external forcing, a GCM produces a considerable amount of low-frequency variability in middle and high latitudes. These results seem to indicate that the observed interannual variations in the occurrence of blocking can to a substantial part be considered as a manifestation of the natural variability of the atmosphere.

In this paper, blocking regimes over the North Atlantic are studied within the context of a spectral 3-level quasi-geostrophic (QG) model. A control experiment and a few sensitivity experiments have been carried out using different external forcing fields. In the control experiment, the QG model is forced by the climatological mean forcing fields of ten winter seasons (1982/83 to 1991/92). The control experiment has been carried out for 500 winters. The ability and limitations of the QG model to produce and maintain the blocking regimes have been investigated. The interannual variations in blocking activity as simulated by the model have been analysed and compared with the observed variability. As the control experiment was carried out with perpetual climatological forcing, the simulated interannual variations can be considered to reflect the natural variability of the model atmosphere.

Observational studies (Lamb and Johnson, 1966; Lamb, 1972; Schuurmans, 1975; Makrogiannis et al., 1982; Bardossy and Caspary, 1990) have shown that blocking activity exhibits significant long-term variations on time scales up to a few decades. The model simulated secular variations in blocking activity have been analysed to determine whether or not these observed long-term variations in blocking activity can be generated internally.

Liu (1994) has shown that a strong zonal flow regime over the Atlantic has approximately the same anomaly pattern as the Atlantic blocking regime but with opposite sign. The average duration of both regimes is about the same. The strong zonal flow regime as simulated by the model has also been analysed and compared with the observations.

The results of the control experiment are presented in Subsection 3.1. In order to investigate the sensitivity of the model simulated blocking activity to the climatological intraseasonal variations in external forcing, we have performed a model experiment in which we include these intraseasonal variations. The results of this experiment are presented in Subsection 3.2. In Section 4, 10 sensitivity experiments are performed to investigate the sensitivity of the model-simulated blocking activity to the precise configuration of the seasonal mean external forcing field. In order to determine the effect of the year-to-year changes in external forcing on the interannual variations in blocking activity, we have integrated the model changing the forcing from one winter to another. The results of this experiment are presented in Section 5. Finally, the summary and conclusions are presented in Section 6.

2. Model description and experimental design

The numerical results described in this paper were obtained using a spectral 3-level quasi-geostrophic model developed by Molteni. The horizontal resolution of the model is triangular 21 (T21). The model has been discussed in detail in Marshall and Molteni (1993). Here we briefly summarize the model equations and the method of deriving the forcing terms of the model. The model integrates prognostic equations for quasi-geostrophic potential vorticity at three levels. The equations have the form:

$$\frac{\partial q_i}{\partial t} = -J(\psi_i, q_i) - D_i + F_i,$$

where the index $i = 1, 2, 3$ refers to the pressure level of 200 hPa, 500 hPa and 800 hPa respectively. q_i is potential vorticity. ψ_i is streamfunction. D_i is a linear operator representing dissipative terms and F_i the forcing term. Potential vorticity q_i is defined as:

$$q_1 = \nabla^2\psi_1 - R_1^{-2}(\psi_1 - \psi_2) + f,$$
$$q_2 = \nabla^2\psi_2 + R_1^{-2}(\psi_1 - \psi_2) - R_2^{-2}(\psi_2 - \psi_3) + f,$$
$$q_3 = \nabla^2\psi_3 + R_2^{-2}(\psi_2 - \psi_3) + f(1 + h/H_0),$$

where $f = 2\Omega \sin \Phi$. R_1 (700 km) and R_2 (450 km) are Rossby radii of deformation appropriate to the 200–500 hPa layer and the 500–800 hPa layer respectively. h is the orographic height and H_0 a scale height (9 km).

The dissipative terms D_i include the contributions from the effects of temperature relaxation with an e-folding time scale of 25 days. Linear drag on the 800 hPa wind with a time scale of 3 days over the oceans, 2 days over the low-altitude land and 1.5 days over mountains above 2 km. A strong scale-selective horizontal diffusion damps harmonics of total wavenumber 21 on a 2 days time scale.

In order to be able to simulate the atmospheric mean state and its variability on various time scales for a certain period, the net forcing acting on the large-scale must be known. Computing the forcing directly from the observations would be a tremendous if not impossible task. We therefore chose a sort of inverse technique as in Roads (1987). Using the observed path in phase space for an extended period of time, assuming that the model is a perfect copy of the atmospheric large-scale circulation and that the net forcing acting on the large-scale circulation can be considered constant over the period, the external forcing can be computed as the residue of the various time-average terms in the equations:

$$F = J(\bar{\psi}, \bar{q}) + D(\bar{\psi}) + \overline{J(\psi', q')},$$

where the overbar denotes a time mean and a prime denotes a deviation from the time mean.

The mean and transient eddy terms representing the external forcing in the control experiment are computed from the daily (12 UTC) European Center for Medium Range Weather Forecasts (ECMWF) streamfunction analyses for a period of 10 winter seasons from 1982/83 to 1991/92. As an example, the external forcing field at 500 hPa is displayed in Fig. 1. It has been converted into a streamfunction forcing and multiplied by $dt = 1$ day. Thus Fig. 1 represents the external forcing applied to the streamfunction fields of the atmosphere per day. In the middle and high latitudes, the external forcing has two negative centers over the Asian and North American continents and two positive centers over the Pacific and Atlantic/European regions. This corresponds well to the main climatological troughs and ridges of the observed atmosphere. Forcing the QG model with this external forcing, a perpetual winter integration has been carried out for 50000 days after a spin-up period of 270 days. These 50000 days are divided into 500 independent winters of 90 days duration by omitting the first 10 days of each 100 day period and retaining the next 90 days. The model output in streamfunction is converted into geopotential height using the linear balance equation.

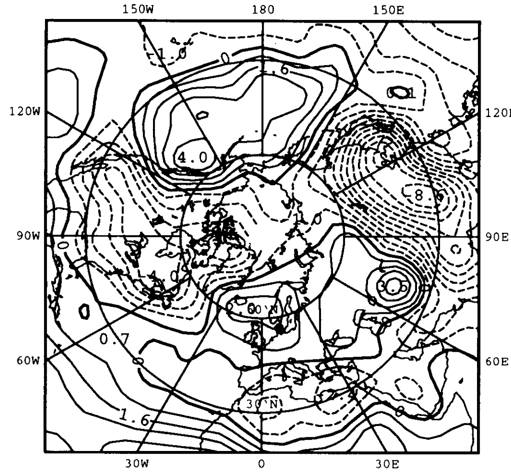

Fig. 1. The climatological mean external forcing for the 10 winter seasons from 1982/83 to 1991/92. It has been converted into a streamfunction forcing and multiplied by $dt = 1$ day. Contour interval 0.8×10^6 m^2/s.

The model results at 500 hPa have been compared with observations. The observational data set contains the Northern Hemisphere daily (12 UTC) 500 hPa geopotential height analyses from the ECMWF for the 10 winter seasons from 1982/83 to 1991/92. The winter season consists of December, January and February. For detailed information about the observed data set, we refer to Liu (1994).

In order to investigate the sensitivity of the model atmosphere to the climatological intraseasonal variations in external forcing, we have performed a model experiment in which we include these intraseasonal variations. The external forcing is computed in the same way as in the control experiment but on a daily basis. For each day of a particular winter, the monthly mean and transient eddy terms representing the monthly mean external forcing centered around that particular day is computed from 31 days of ECMWF analyses. For example, the forcing centered around 1 December 1982 is computed from the ECMWF streamfunction analyses of 15 November to 15 December 1982. The climatological mean external forcing for a particular day is then computed by averaging the forcing fields of that day over the 10 observed winters. The model experiment has been carried out for 100 independent winters. A winter contains 90 days, each of them is forced by the climatological mean external forcing for that particular day.

In Section 4, the results of ten sensitivity experiments are described that have been performed to investigate the sensitivity of the model simulated blocking activity to the precise potential vorticity forcing configuration. Instead of using the climatological mean forcing fields we compute the forcing fields for the 10 individual winter seasons of 1982/83 to 1991/92. Forcing the model with the forcing fields of each of the individual winters, ten experiments have been performed. Each of them has been carried out for 10000 days and, similar to the control experiment, from this data set 100 independent winters of 90 days duration were formed.

In order to investigate the effect of the year to year changes in external forcing on the interannual variations in blocking activity, we ran the model with the forcing changing from one winter to another in Section 5. For the forcing fields we randomly pick one of the ten observed forcing fields as computed for the winter seasons of 1982/83 to 1991/92 and generate a data set of 500 independent winters. In practice, we randomly select 500 simulated winters from the ten sensitivity experiments as described above and consider this one possible realisation of a time series of 500 independent winters.

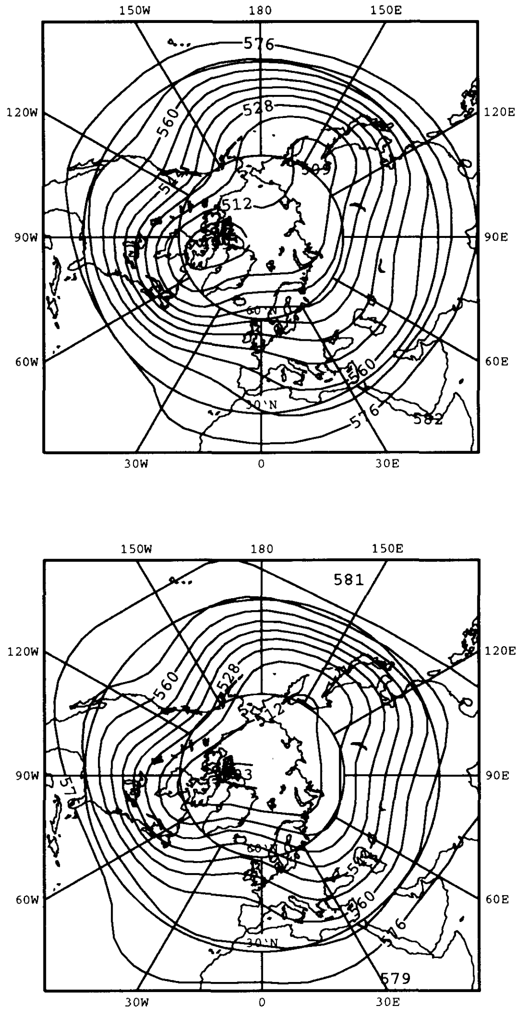

Fig. 2. Northern Hemisphere mean 500 hPa geopotential height fields for (a) observations and (b) model simulation. Contour interval 80 m.

3. Climatological forcing

3.1. Perpetual climatological forcing: the control experiment

3.1.1. Comparison of observed and simulated statistics. Fig. 2a, b shows the observed and model simulated mean 500 hPa geopotential height fields for the Northern Hemisphere. The observed planetary-scale stationary features are well reproduced. The main climatological troughs and ridges are in the right position and have approximately the correct amplitudes. Fig. 3 shows the observed and simulated standard deviations of the daily 500 hPa geopotential heights. There is general agreement in the overall structure of the variance fields. The model is able to simulate the maxima over the Pacific and Atlantic ocean. There are, however, some deficiencies. The simulated Pacific maximum is slightly too strong and the Atlantic

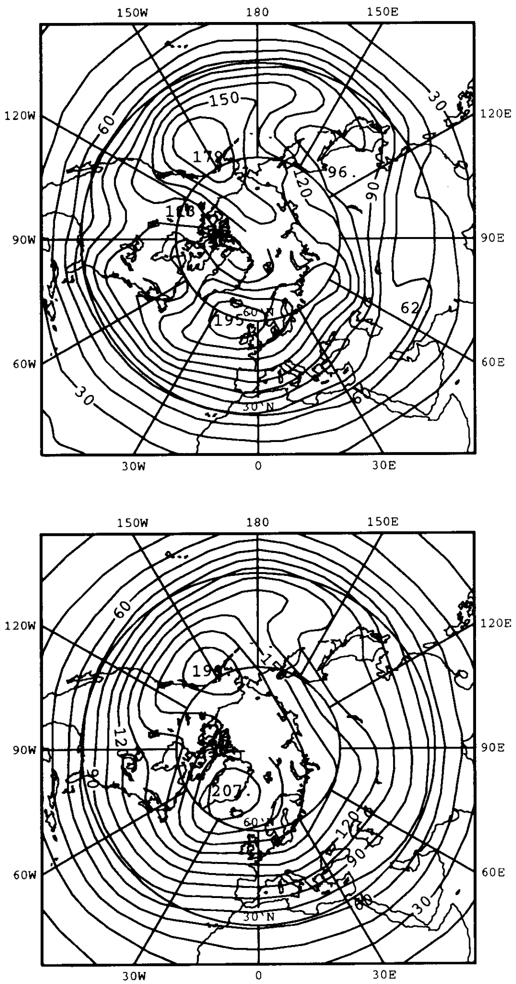

Fig. 3. Northern Hemisphere standard deviation of daily geopotential height at 500 hPa for (a) observations and (b) model simulation. Contour interval 15 m.

maximum is located too far to the north. The simulated high and low-frequency variance patterns and the principal empirical orthogonal functions (EOFs) at 500 hPa have also been computed (not shown). They are all in good agreement with their observed counterparts.

Liu (1994) has shown that observed blocking is associated with large positive 500 hPa geopotential height anomalies and strong zonal flow with large negative anomalies centered at about 60° N. The longitudinal distribution of large positive and negative 500 hPa geopotential height anomalies at 60° N has been computed for the observations and model simulation. For each day of the observations and model simulation, the geopotential height anomaly from the corresponding climatological mean has been computed at each longitudinal point at 60° N. We call this time series ZA60(λ), where λ represents longitude. Fig. 4a, b, respectively, show the mean number of days per winter that satisfy ZA60(λ) $\geqslant$ 100 m and ZA60(λ) $\leqslant -100$ m as a function of λ. The solid line is for the observations and the dashed line for the model simulation. The model reproduces approximately the observed longitudinal distribution of large geopotential height anomalies at 60° N. Particularly, it simulates the two preferred regions for blocking and strong zonal flow over the northeastern Atlantic and northeastern Pacific with only minor deficiencies. The discrepancy with the observations is relatively small and may partly be attributed to sampling errors of the observational data set, as we are comparing a 500-winter model simulation with only a 10-winter observational data set. We will discuss this sample problem in detail in Subsection 3.1.5.

3.1.2. Structure of the model simulated blocking. Liu (1994) has investigated the spatial structure of the observed Atlantic blocking by analyzing the composite mean and anomalies in 500 hPa geopotential height for the days with large positive geopotential height anomalies at 60° N. The same analysis technique has been applied to the model simulation. For each model day, the latitudinal mean anomaly of 500 hPa geopotential height over the Atlantic and western European areas has been computed at 60° N. We call it ZA60. It is computed by averaging the daily geopotential height anomalies at 16 grid points from about 55° W to 30° E:

$$\mathrm{ZA60} = \frac{\sum_{i=1}^{16} \mathrm{ZA60}(i)}{16},$$

where $i = 1$ to 16 represents longitudinal points of $\lambda = 55°$ W to 30° E.

In the same way as in Liu (1994), 10000 days (out of 45000 days) with the largest positive anomalous values of ZA60 have been selected. The mean state of these 10000 days and its anomalies from the climatological mean of the model simulation are shown in Fig. 5a, b. They are very similar to the fields derived from the above mentioned

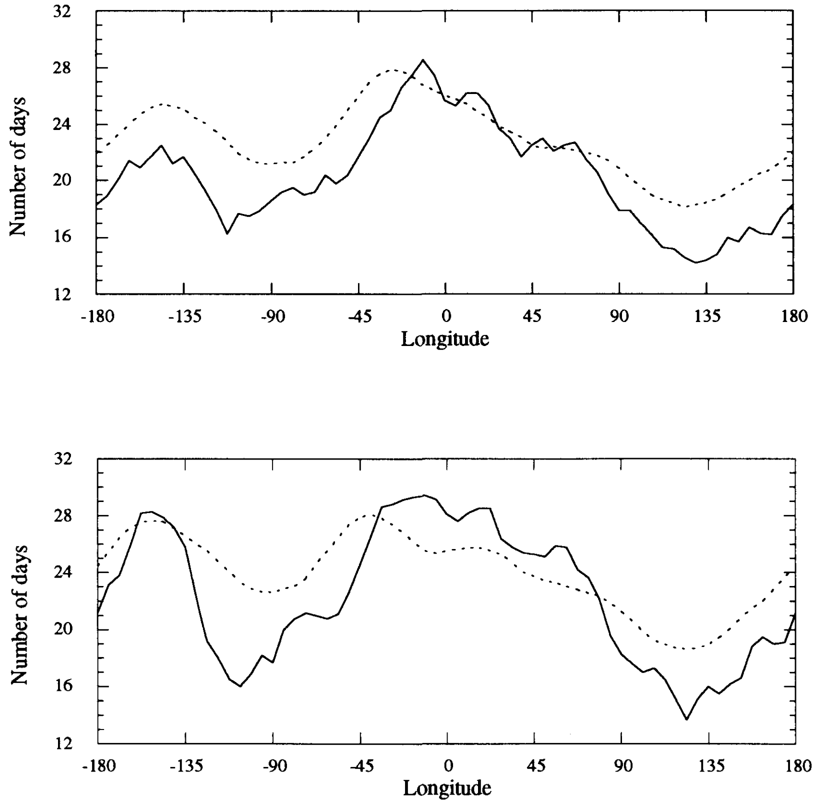

Fig. 4. Number of days per winter that satisfy (a) ZA60(λ) $\geqslant$ 100 m and (b) ZA60(λ) $\leqslant -100$ m as a function of longitude. The solid line is for observations and the dashed line for the model simulation.

observational data set (Fig. 2a, b of Liu, 1994). Fig. 5a displays the typical blocking pattern of Rex (1950) over the North Atlantic ocean. The center of the blocking high is located at about 50° N. The anomaly pattern of Fig. 5b is dominated by a strong positive anomaly centered at about 60° N and a negative anomaly south of it. It has also approximately the same amplitude as the observed anomaly pattern. The band-pass filtered (2 to 6 days) standard deviation of the daily 500 hPa geopotential heights for these 10000 days has been computed (not shown). We find that the activity of the transient weather disturbances is weakened near the center of the blocking high and enhanced north of it. This is also in agreement with observations (Liu, 1994). So it appears that the QG model simulates quite well the blocking pattern as well as its effect on the transient disturbances.

Fig. 6a, b shows the composite mean and anomalous 500 hPa geopotential height field for the 10000 days with the largest negative anomalous values of ZA60. Again, they are in very good agreement with observations (Liu, 1994). The mean field is a typical high zonal index flow over the North Atlantic and western European areas. The simulated strong zonal flow regime has approximately the same anomaly pattern as the blocking regime but with opposite sign. It is characterized by a large negative anomaly centered at 60° N and a positive anomaly south of it.

3.1.3. The frequency and persistence of the model simulated blocking. As blocking and strong zonal flow regimes over the North Atlantic and western European areas are associated with approximately the same anomaly pattern with opposite sign, a single blocking index is used to measure the resemblance of a particular circulation pattern with the blocking regime or the strong zonal flow regime. To do this, each of the daily 500 hPa geopotential height anomaly fields has been projected onto the

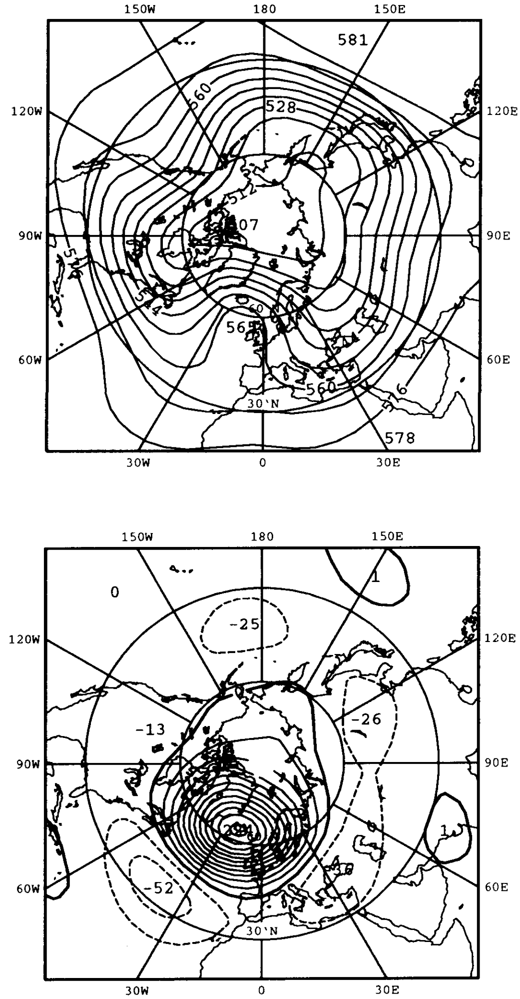

Fig. 5. (a) The mean and (b) its anomalies from the climatological mean of the 500 hPa geopotential height for the 10000 days with the largest positive anomalous values of ZA60. Contour interval is 80 m in (a) and 20 m in (b).

simulated blocking anomaly pattern of Fig. 5b. The projection area is the Atlantic-European area from 10° N to 85° N and from 90° W to 60° E. We call it blocking index (BINX). Following Liu (1994), the blocking index is defined as:

$$\mathrm{BINX} = \frac{\langle z_b, z_d \rangle}{\langle z_b, z_b \rangle}.$$

where z_b is the blocking anomaly field in geopotential height and z_d the daily geopotential height anomaly field. The angle brackets denote a squared norm inner product. To filter out the brief transient interruption, the blocking index has been smoothed by applying a 5-day running mean smoother.

Table 1 gives the total number of blocking days and events for the model simulation, normalized to 10 winters. A blocking day is defined as a day with $\mathrm{BINX} \geqslant 0.5$ and a blocking event is defined as a period of consecutive days for which $\mathrm{BINX} \geqslant 0.5$. For comparison, the number of blocking days and events for the observations are also given in Table 1. They are computed from the 5-day running mean blocking index data for the observed 10-winter period (Liu, 1994). Note that in order to achieve consistency, the blocking index for the observations is computed by projecting the daily geopotential height anomaly fields onto the observed blocking anomaly pattern (Fig. 2b in Liu, 1994). This observed blocking anomaly pattern differs slightly from the simulated blocking anomaly pattern of Fig. 5b. However, this difference is very small. Table 1 shows that the QG model produces approximately the same number of blocking days as observed in the 10-winter period. However, the model produces too many short-lived blocking events and consequently, the average duration of the simulated blocking regimes (8.1 days) is about one day shorter than the observed one (9.3 days).

The same analysis has been applied for the strong zonal flow regime ($\mathrm{BINX} \leqslant -0.5$). The results are summarized in Table 2. Again, the model produces approximately the same number of strong zonal flow days as observed, but the average duration of the simulated strong zonal flow regimes is about one and half day shorter than the observed one. Also, the model produces approximately the same number of blocking and strong zonal flow days.

Table 1. *Number of blocking days and events ($BINX \geqslant 0.5$, normalized to 10 winters), and the average duration of the blocking regimes in observations and the control experiment*

	Observations	Model
no. blocking days	233	226
no. blocking events	25	28
average duration of blocking	9.3	8.1

Table 2. *Number of strong zonal flow (SZF) days and events ($BINX \leqslant -0.5$, normalized to 10 winters), and the average duration of the strong zonal flow regimes in observations and the control experiment*

	Observations	Model
no. SZF days	242	229
no. SZF events	26	30
average duration of SZF	9.3	7.6

This corresponds to the results for the observed 10 winters dataset (Liu, 1994). We notice that the model simulated strong zonal flow regime is slightly less persistent than the simulated blocking regime. However, the difference is small (0.5 days).

Computations have also been done using different blocking index threshold values from 0.6 to 0.9. Still, the model produces approximately the same number of blocking and strong zonal flow days as in the observations and the average duration of the simulated regimes is slightly shorter than the observed. To test the sensitivity of our results to small changes in the structure of the blocking anomaly pattern, we have also projected the daily anomaly patterns to the strong zonal flow anomaly pattern of Fig. 6b. The results remain almost identical as summarized in Table 1 and 2.

Summarizing, the QG model produces approximately the same number of blocking days as in the observations. However, the probabilities for long lasting regimes are substantially lower than in the observations. This discrepancy may partly be attributed to sampling errors in the 10-year dataset. As can be shown both from observations and our model simulation, there exists substantial decadal variability in the occurrence and persistence of blocking.

3.1.4. The interannual and decadal variations in blocking activity. Fig. 7a, b displays, for observations and the first 10 winters of model simulation, the number of blocking ($BINX \geqslant 0.5$) and strong zonal flow ($BINX \leqslant -0.5$) days over the North Atlantic and western European areas per winter. It is evident that the interannual variations in blocking and strong zonal flow activity are substantial both in the observations and the model results. From the 10 observed winters, the 1989/90 winter has the lowest number of blocking days (8),

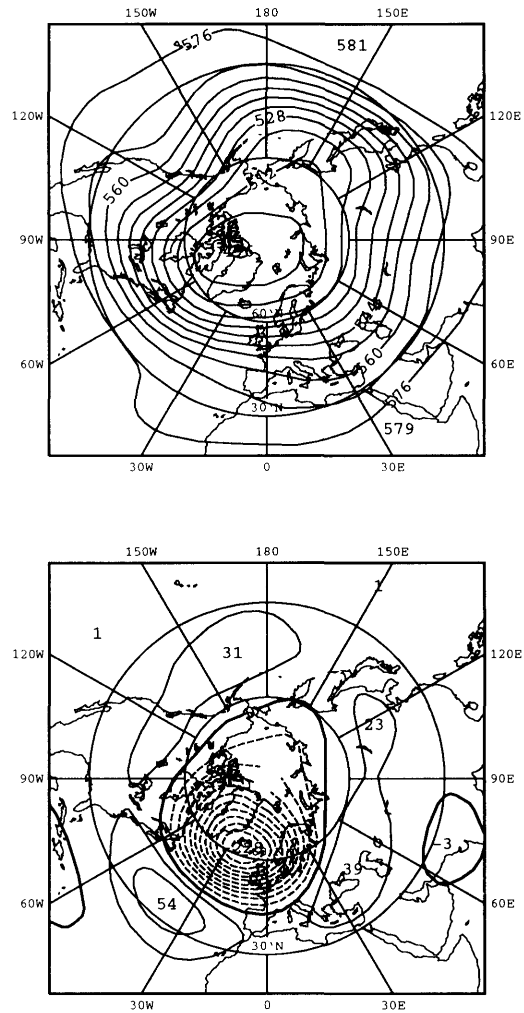

Fig. 6. Same as Fig. 5, but for the 10000 days with the largest negative anomalous values of ZA60.

while the winter of 1991/92 has 39 days of blocked flow. The mean of the 10 observed winters is 23.3 blocking days with a standard deviation of 10.4 days. For the model simulation, the number of blocking days varies from 3 days in model winter 8 to 36 days in model winter 5. The mean of the 10 model winters is 14.7 blocking days with a standard deviation of 11.3 days. For the entire period of 500 model winters, the number of blocking days of each winter varies from 0 to 82 days. The mean is 22.6 blocking days and the standard deviation is 15.3 days.

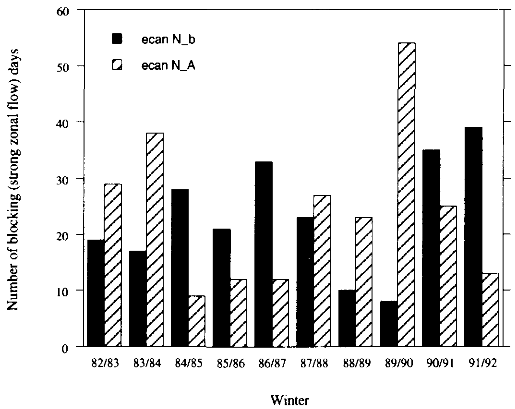

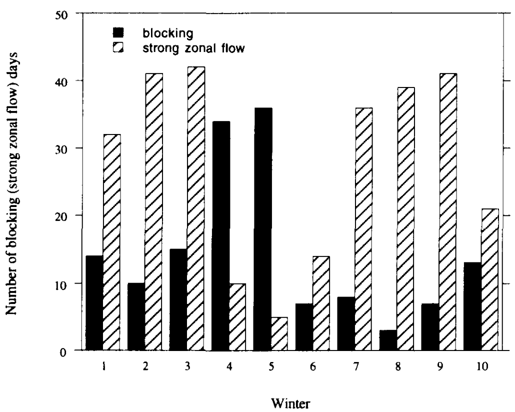

Fig. 7. The number of blocking and strong zonal flow days per winter over the North Atlantic and western Europe for (a) observations and (b) the first 10 winters of the model simulation.

Observational studies (Lamb and Johnson, 1966; Lamb, 1972; Schuurmans, 1975; Makrogiannis et al., 1982; Bardossy and Caspary, 1990) have shown that the occurrence of blocking exhibits long-term variations on various time scales up to a few decades. These studies indicate that blocking activity over North Atlantic has been relatively frequent in the last 20 years of the 19th century and since about 1950, with more zonal circulations predominating in the intervening period. Fig. 8 shows, for the 500 winters of the model simulation, the number of blocking days over the North Atlantic and western European areas per winter. The dashed line represents the number of blocking days at each winter. The thick solid line is the 11-year running mean. The thin solid line represents the average number of blocking days per winter for the whole period of 500 model winters (22.6 days). Fig. 8 shows that while the number of blocking days exhibits strong random fluctuations from one winter to another, long-term variations in blocking activity occur on various time scales up to a few decades which are similar to the observed variations. For example, the model has generated a period of about 40 winters (from about model winter 45 to winter 85) with stronger than normal blocking activity and a period of about 50 winters (from about model winter 200 to 249) with weaker than normal blocking activity. The average number of blocking days per winter is about 30 during the first period and 18 during the second period. The decadal variations in blocking activity are even larger. For the 11-year running mean data, the average number of blocking days per winter varies from 13.5 days in model winter 434 to 444 to 38.3 days in model winter 66 to 76. Power spectrum analysis (not shown) indicates that the simulated fluctuations in the number of blocking days can be represented approximately as a white noise process. So it is not necessary to assume some very low-frequency anomalous forcing to explain decadal variability in blocking activity.

Fig. 9 shows the secular variation in blocking duration for the 500-winter model simulation. The dashed line represents the average duration of blocking at each winter. The thick solid line is the 11-year running mean. The thin solid line represents the climatological mean blocking duration of the model simulation (8.1 days). Again, long-term variations in blocking duration occur on various time scales up to a few decades. For the 11-year running mean data, the average duration of the blocking regimes varies from 4.9 days in model winter 289 to 299 to 16.9 days in model winter 263 to 273.

As the QG model accurately simulates the observed blocking structure as well as the interannual and decadal variations in blocking activity without any anomalously imposed external forcing, we conclude that blocking is predominantly an internally generated phenomenon. However, this result does not exclude the possibility that interannual variations in external forcing are also significantly contributing to the interannual variations in blocking activity. We will investigate this in the following sections.

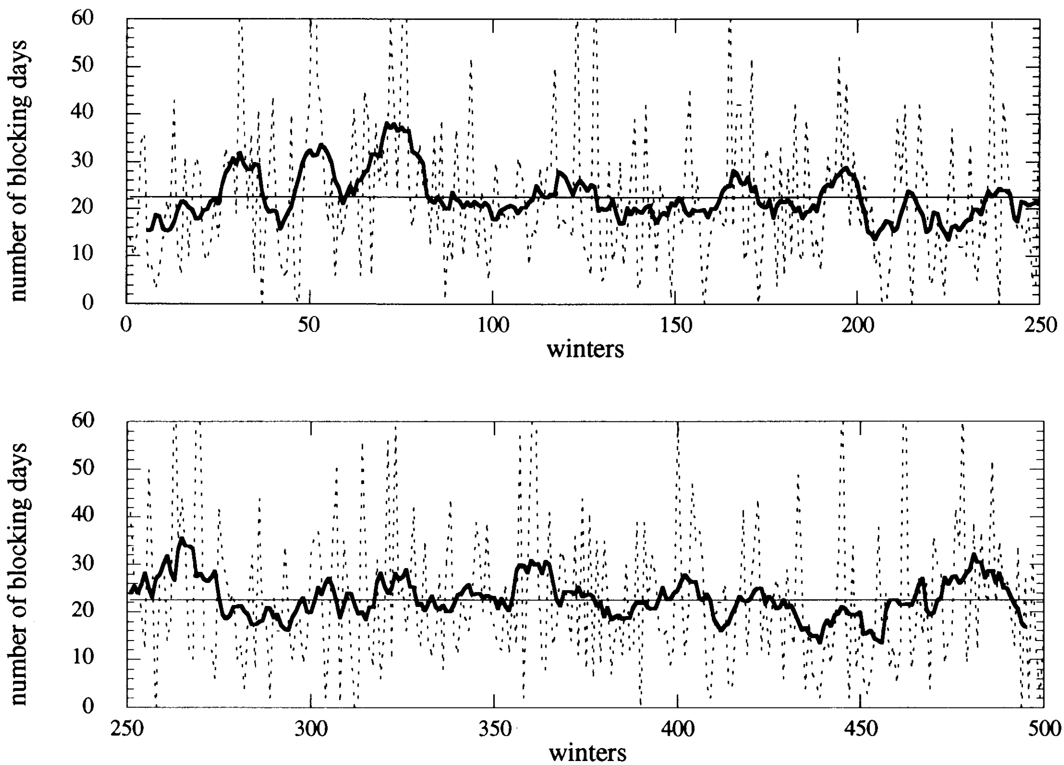

Fig. 8. The number of blocking days per winter for the 500 winters control run. The dashed line represents the number of blocking days at each winter. The thick solid line is the 11-year running mean. The thin solid line represents the average number of blocking days per winter for the whole period of 500 model winters.

3.1.5. Discussion of GCM results. The simulation of blocking in GCMs has been examined in many studies. While all of these studies have demonstrated that GCMs can produce realistic blocking patterns, they disagree with respect to the ability of GCMs to reproduce the observed climatology of blocking. Shukla et al. (1981) found that the climate model of the Goddard Laboratory for Atmospheric Sciences does not simulate the location, intensity and duration of the observed blocking events. Mansfield (1981) examined the blocking in the British Meteorological Office GCM. He showed that the model reproduces the observed distributions of blocking in both time and space. The main failing in the model is its inability to maintain blocking. Blackmon et al. (1986) examined blocking in a 1200-day perpetual January run of the NCAR's Community Climate Model. They showed that the model reproduces the observed persistence of blocking over the Atlantic and Pacific oceans. It also produces a realistic number of blocking events over the Pacific ocean. However, the model does not produce the observed number of blocking events over the Atlantic ocean. Dugas and Derome (1992) noticed that the Canadian Climate Center GCM can not simulate the correct frequency of the occurrence of persistent anomalies. Anderson (1993) showed that for the winter season, the Medium-Range Forecast Model of the U.S. National Meteorological Center produces a realistic number of blocking events over the Atlantic and Pacific oceans, and the simulated blocking events persist slightly longer than the observed blocking events.

While many possible factors have been suggested for causing the different results of the above GCM experiments (Shukla, 1982; Tibaldi and Molteni, 1990; Anderson, 1993), it is important to bear in mind that only relatively small samples of data have been analysed in the above mentioned studies. We have shown that even without any anomalously imposed external forcing, a QG

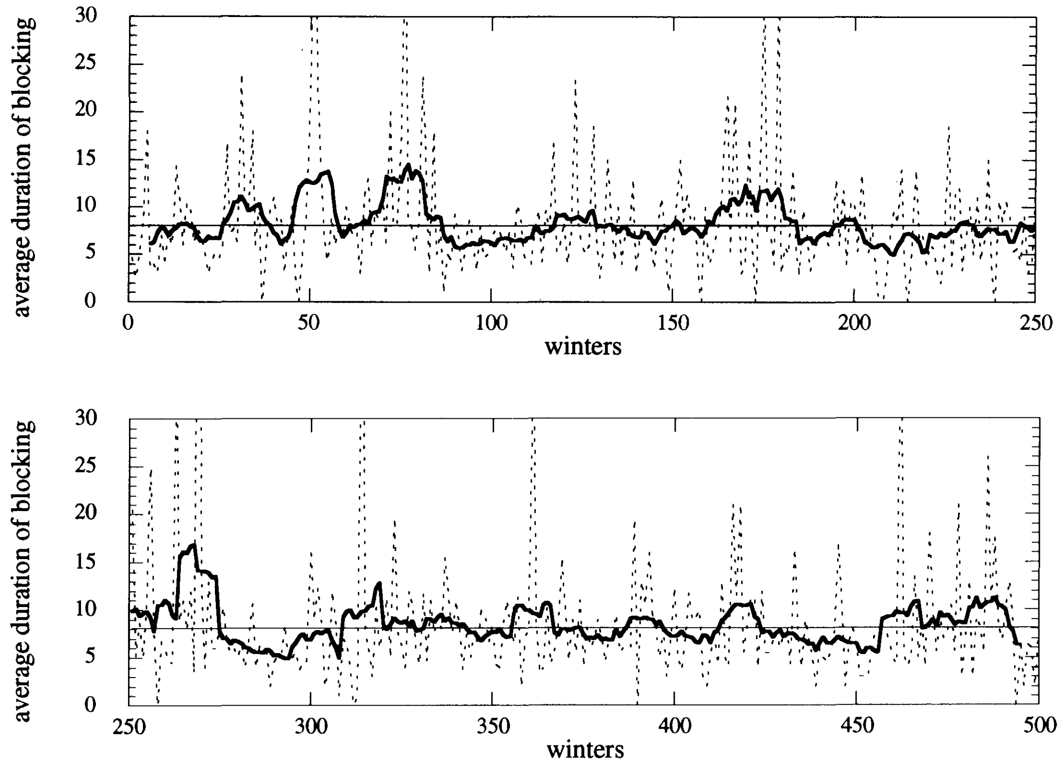

Fig. 9. The average duration of the blocking regimes at each winter for the control experiment. The dashed line represents the average duration of blocking at each winter. The thick solid line is the 11-year running mean. The thin solid line represents the climatological mean blocking duration of the model simulation.

model internally generates substantial decadal variations in blocking activity. This is not only true for the number of blocking days, but also for the mean duration of blocking. As the observed and GCM simulated data sets of the above mentioned studies are in general not much longer than a decade, the controversial results may partly be caused by unrepresentative sampling and can not totally be attributed to model errors or errors in the boundary conditions.

3.2. The inclusion of the climatological intraseasonal variations in forcing

In order to investigate the sensitivity of the model atmosphere to the climatological intraseasonal variations in external forcing, we performed a model experiment in which we included these intraseasonal variations. As described in Section 2, we computed the climatological mean external forcing fields on a daily basis. The model experiment has been carried out for 100 independent winters. A winter contains 90 days, each of them is forced by the climatological mean external forcing for that particular day. The model simulated a mean of 23.0 blocking days per winter with a standard deviation of 14.4 days. This is almost the same as in the control experiment. It also generated almost the same decadal variations in blocking activity as in the control experiment. So with respect to the mean and interannual variations in blocking activity, the effect of intraseasonal variations in external forcing is negligible.

4. Impact of the seasonal mean forcing

We next investigated the sensitivity of the model simulated blocking activity to the precise potential vorticity forcing configuration. Instead of using the climatological winter mean forcing field, we have forced the model with the forcing fields of the ten individual winters. Each of the ten experiments has been carried out for 100 independent winters.

For each of the ten experiments the blocking index is computed by projecting the daily 500 hPa geopotential height anomaly fields (with respect to the climatological mean state of the control run) onto the blocking anomaly pattern of Fig. 5b. Same as in the control experiment, the blocking index is smoothed by applying a 5-day running mean smoother and the number of days satisfying BINX $\geqslant 0.5$ has been computed for each of the ten experiments.

The number of blocking days simulated in these experiments are given in Table 3. There are large differences in model simulated blocking activity. The model simulates a mean of 15.1 blocking days per winter when it is forced by the forcing field of the 1983/84 winter, and a mean of 48.6 blocking days per winter when it is forced by the forcing field of the 1987/88 winter. This result indicates that blocking in the quasi-geostrophic model is sensitive to the forcing configuration and that changes in the forcing can have quite a substantial impact on the probability for blocking to occur. Comparing the simulated mean number of blocking days for the ten winters with the actually observed number of blocking days in those winters, it appears that 6 of the 10 are within one standard deviation from the simulated mean. This is what can be expected if we do a random drawing from the simulated data set for those ten years. So the model results of Table 3 are not contradicted by the observations.

The strong sensitivity of the model simulated blocking activity to the forcing configuration as demonstrated in this section does not necessarily mean that the interannual variations in external forcing will significantly change the interannual variability in blocking activity as compared to the result for the climatological seasonal mean forcing. As shown in Table 3, each of the experiments also generates strong interannual variations in blocking activity and is carried out for 100 winters keeping the forcing constant. In reality, the external forcing is changing from one winter to another. We have investigated to what extent interannual variations in the seasonal mean forcing affect the mean number of blocking days and its interannual variability. The results are described in the following section.

Table 3. *The mean and interannual variations in blocking activity simulated in the 10 sensitivity experiments; these experiments are forced with the forcing fields of each of the 10 individual winter seasons of 1982/83 to 1991/92*

	Blocking days per winter	Standard deviation
82/83	20.7	10.8
83/84	15.1	12.1
84/85	37.3	18.4
85/86	23.5	14.3
86/87	16.6	11.2
87/88	48.6	16.2
88/89	39.6	18.2
89/90	23.3	15.3
90/91	25.9	13.8
91/92	20.1	13.9

5. Interannual variations in the forcing

In order to investigate the effect of the year to year changes in external forcing on the interannual variations of blocking activity, we performed a model experiment with the forcing changing from one winter to another. This is done by randomly selecting 500 simulated winters from the ten sensitivity experiments of Section 4 and consider this as one realisation of a time series of 500 independent winters.

Again, the blocking index is computed by projecting the daily 500 hPa geopotential height anomaly fields (with respect to the climatological mean state of the control run) onto the blocking anomaly pattern of Fig. 5b. Using the same process and the same blocking index criteria as in the control experiment, the average number of blocking days and the interannual variations in blocking activity are computed. The results are given in Table 4 together with the results of the control experiment. The mean number of blocking days of this experiment (27.3 days per winter) is

Table 4. *The mean and interannual variations in blocking activity in the control experiment and the experiment including the year to year changes in external forcing (perturbation experiment)*

	Blocking days per winter	Standard deviation
control experiment	22.6	15.3
perturbation experiment	27.3	17.2

larger than that in the control experiment (22.6 days per winter). This may partly be due to the fact that in the control experiment, the strength of the external forcing is weakened by averaging the forcing fields for ten winters. The model also generates more blocking than in the observations. However, the observed mean number of blocking days (23.3 days per winter) is well within one standard deviation from the simulated mean (27.3 ± 5.8 days per winter). The standard deviation of 5.8 days is derived from the 500 winters dataset by dividing it into 50 periods of 10 winters. It is then computed from the average number of blocking days per winter for each of the 10-winter periods.

Including the year to year changes in external forcing, the model generated slightly larger interannual variations in blocking activity (17.2 days) as compared to the control experiment (15.3 days). However, the change is relatively small. So although the external forcing does have a substantial impact on the probability for blocking to occur, the interannual variations in forcing do not strongly change the interannual variability in blocking activity as compared to the experiment with constant climatological forcing. It seems that the observed interannual variability of blocking in winter is predominantly internally generated and changes in external forcing have only a small modifying effect.

The model also generated almost the same decadal variations in blocking activity as in the control experiment. The experiment has been repeated for ten times with different samples of 500 random winters. They all result in the same conclusion.

6. Summary and conclusions

Blocking regimes simulated in a spectral 3-level QG model have been examined and compared with observations. The main emphasis of this paper is to determine the relative importance of changes in external forcing and internal dynamics of the model atmosphere for causing interannual variations in the occurrence of blocking over the North Atlantic.

Forcing the model with the climatological winter mean external forcing, a control experiment has been carried out for 500 winters. The model simulates accurately the structure of the Atlantic blocking pattern, as well as its effect on the transient weather systems. It also produces approximately the same number of blocking days as in the observations. However, the average duration of the simulated blocking regimes is about one day shorter than the observed one. This may be partly due to sampling problems caused by the rather short observational data set.

The same analysis has been applied to the strong zonal flow regime. The model also produces approximately the correct number of strong zonal flow days, but again the average duration of the simulated strong zonal flow regime is shorter than observed. The model simulated strong zonal flow has approximately the same anomaly pattern as the simulated blocking regime but with opposite sign. Also, the model simulates approximately the same number of blocking and strong zonal flow days and the difference between the average duration of the blocking and strong zonal flow regimes is very small. This is in agreement with the results for the observations (Liu, 1994).

We have shown that the interannual variability in blocking activity of the control experiment is similar to the observations. It also produces substantial long-term variations in blocking activity on a time-scale of decades. As the QG model reproduces the observed blocking phenomenon as well as the interannual and decadal variations in blocking activity without any anomalously imposed external forcing, we conclude that blocking is to a large extent an internally generated phenomenon. This is even true for the observed secular variations in blocking activity.

We have investigated the sensitivity of the model atmosphere to the climatological intraseasonal variations in external forcing. With respect to the mean number of blocking days and interannual variations in blocking activity, the contribution of intraseasonal variations in external forcing is negligible.

Ten sensitivity experiments have been carried out which are forced by the forcing fields of each of the ten individual winters of 1982/83 to 1991/92. We found that blocking in the quasi-geostrophic model is sensitive to the seasonal mean forcing configuration and that changes in the forcing can have quite a substantial impact on the probability for blocking to occur.

In order to investigate the effect of the year to year changes in external forcing on the interannual variations of blocking activity, we performed a model experiment with the forcing changing from one winter to another. Including the year to year changes in seasonal mean external forcing, the model generates slightly larger interannual variations in blocking activity as compared to the control experiment. However, the effect is relatively small. We therefore conclude that blocking in winter is predominantly an internally generated phenomenon and that changes in external forcing have a relatively small modifying effect on the interannual variability of blocking.

7. Acknowledgments

We would like to thank Cor Schuurmans, Reindert Haarsma and Robert Mureau for their valuable comments and constructive criticisms on this paper. Thanks are also due to Franco Molteni for providing his model and to Jan Barkmeijer, Peter Houtekamer, Frank Selten and Xueli Wang for their assistance in executing the numerical experiments. This study is supported by the working group on Meteorology and Physical Oceanography (MFO) with financial aid from the Netherlands Organization for Scientific Research (NWO).

REFERENCES

Anderson, J. L. 1993. The climatology of blocking in a numerical forecast model. *J. Climate* **6**, 1041–1056.

Bardossy, A. and Caspary, H. J. 1990. Detection of climate change in Europe by analyzing European atmospheric circulation patterns from 1881 to 1989. *Theor. Appl. Climatol.* **42**, 155–167.

Blackmon, M. L., Mullen, S. L. and Bates, G. T. 1986. The climatology of blocking events in a perpetual January simulation of a spectral general circulation model. *J. Atmos. Sci.* **43**, 1379–1405.

Chervin, R. M. 1986. Interannual variability and seasonal climate predictability. *J. Atmos. Sci.* **43**, 233–251.

Dugas, B. and Derome, J. 1992. On the climatology of persistent circulation anomalies in the atmosphere and in a general circulation model. *Atmosphere-Ocean* **30**, 339–361.

Lamb, H. H. 1972. British Isles weather types and a register of the daily sequencies of circulation pattern 1861–1971. *Geophys. Memoris*, no. 116, London.

Lamb, H. H. and Johnson, A. I. 1966. Secular variations of the atmospheric circulation since 1750. *Geophys. Memoris*, no. 110, London.

Lau, N.-C. 1981. A diagnostic study of recurrent meteorological anomalies appearing in a 15-year simulation with a GFDL general circulation model. *Mon. Wea. Rev.* **109**, 2287–2311.

Liu, Q. 1994. On the definition and persistence of blocking. *Tellus* **46A**, 286–298.

Makrogiannis, T. J., Bloutsos, A. A. and Giles, B. D. 1982. Zonal index and circulation change in the North Atlantic area, 1883–1972. *Journal of Climatology* **2**, 159–169.

Manabe, S. and Hahn, D. G. 1981. Simulation of atmospheric variability. *Mon. Wea. Rev.* **109**, 2260–2286.

Mansfield, D. A. 1981. *The incidence of blocking in the Meteorological Office's 5-level model.* Met. O. 13 Branch Memorandum No. 99, Meteorological Office, Bracknell.

Marshall, J. and Molteni, F. 1993. Toward a dynamical understanding of planetary-scale flow regimes. *J. Atmos. Sci.* **50**, 1792–1818.

Mullen, S. L. 1989. Model experiments on the impact of Pacific sea surface temperature anomalies on blocking frequency. *J. Climate* **2**, 997–1013.

Namias, J. 1964. Seasonal persistence and recurrence of European blocking during 1958-1960. *Tellus* **16**, 394–407.

Rex, D. F. 1950. Blocking action in the middle troposphere and its effect upon regional climate (I). An aerological study of blocking. *Tellus* **2**, 196–211.

Roads, J. O. 1987. Predictability in the extended range. *J. Atmos. Sci.* **44**, 3495–3527.

Schuurmans, C. J. E. 1975. On the relation between polar activity and the occurrence of blocking-type circulation. *Proceedings of the WMO/IAMAP symposium on long-term climatic fluctuations*. Norwich, 18–23 August 1975, pp. 265–266.

Shukla, J. 1982. Ability and limitations of general circulation models to simulate climate and climate variability. *WMO/ICSU Study Conference on the Physical basis for climate prediction on seasonal, annual and decadal time scale*. Leningrad (USSR), 13–17 September 1982, pp. 97–127.

Shukla, J., Mo, K. C. and Eaton, M. 1981. *Climatology of blocking in the GLAS climate model.* NASA Tech. Memo. No. 83907, pp. 207–216.

Tibaldi, S. and Molteni, F. 1990. On the operational predictability of blocking. *Tellus* **42A**, 343–365.

White, W. B. and Clark, N. E. 1975. On the development of blocking ridge activity over the central North Pacific. *J. Atmos. Sci.* **32**, 489–502.